Uncovering Early Galaxy Evolution in the ALMA and JWST Era
Proceedings IAU Symposium No. 352, 2019
E. da Cunha, J. Hodge, J. Afonso, L. Pentericci & D. Sobral, eds.

doi:10.1017/S1743921320000708

Synthetic nebular emission lines of simulated galaxies over cosmic time

Michaela Hirschmann

DARK, Niels Bohr Institute, University of Copenhagen, Lynbyvej 2, 2100 Copenhagen, Denmark
email: michaela.hirschmann@nbi.ku.dk

Abstract. This article presents an up-dated analysis of synthetic optical and UV emission lines of simulated galaxies over cosmic time. The strong emission lines are derived from self-consistently coupling novel spectral models accounting for nebular emission from young stars, AGN and Post-AGB stars to cosmological zoom-in as well as large-scale simulations. Investigating the evolution of optical line-ratios in the BPT diagrams, the simulations can successfully reproduce the observed trend of [OIII]/Hβ ratio increasing from low to high redshifts, due to evolving star formation rate and gas metallicity. Standard selection criteria in the BPT diagrams can appropriately distinguish the main ionising source(s) of galaxies at low redshifts, but they are less reliable for metal-poor galaxies, dominating the early Universe. To robustly classify the ionising radiation of such metal-poor galaxies, diagnostic diagrams based on luminosity ratios of UV lines are discussed. The novel interface between simulations and observations is potentially important for the interpretation of high-quality spectra of very distant galaxies to be gathered by next-generation telescopes, such as the James Webb Space Telescope.

Keywords. methods: numerical, galaxies: evolution, galaxies: formation, galaxies: high-redshift, galaxies: ISM, (galaxies:) quasars: emission lines

1. Introduction

The emission from ionized interstellar gas contains valuable information about the nature of the ionizing radiation and the physical conditions in the interstellar medium (ISM) in a galaxy. In fact, prominent optical emission lines are routinely used to estimate the density, chemical abundances and dust content of the ISM and whether ionization is dominated by young massive stars (tracing the star formation rate hereafter SFR), an active galactic nucleus (hereafter AGN) or evolved, post-asymptotic giant branch (hereafter post-AGB) stars (e.g. Izotov *et al.* (1999); Kauffmann *et al.* (2003); Kewley & Ellison (2008); Morisset *et al.* (2016)). One of the most widely used line-ratio diagnostic diagrams, originally defined by Baldwin, Phillips & Terlevich (1981, hereafter BPT), relate the [OIII]λ5007/Hβ ratio to the [NII]λ6584/Hα ratio, allowing for an identification of the nature of the ionizing radiation in large samples of galaxies in the local Universe (e.g. Kewley *et al.* (2001); Kauffmann *et al.* (2003)).

Interestingly, several recent observational studies indicate that star-forming (SF) galaxies at z $>$ 1 have systematically larger [O III]/Hβ ratios, at fixed [N II]/Hα ratio, than their present-day counterparts from the Sloan Digital Sky Survey (SDSS; see e.g. Yabe *et al.* (2014); Steidel *et al.* (2014); Shapley *et al.* (2015); Strom *et al.* (2017)). The physical origin of this intriguing observational feature is being heavily debated and several explanations have been proposed (higher ionisation parameter, higher electron density, contribution from AGN, harder ionising radiation from stars).

In addition, at the very low metallicities expected in the youngest galaxies at high redshifts (e.g. Maiolino *et al.* (2008)), emission-line ratios for SF- and AGN-dominated models tend to occupy similar regions of the [OIII]/Hβ–[NII]/Hα diagram (Feltre *et al.* (2016)) so that their usefulness to constrain the nature of ionizing sources in the early universe is uncertain. In recent years, interest has grown in ultraviolet (UV) nebular emission lines, such as CIII]λ1908, CIVλ1550, and HeIIλ1640 lines, which tend to be particularly prominent in metal-poor, actively SF dwarf galaxies at all redshifts (e.g. Stark *et al.* (2014); Berg *et al.* (2016)).

To reach more specific conclusions on the (i) origin of the evolution of optical line-ratios, and (ii) how to best identify the main ionising sources in metal poor galaxies requires the self-consistent modelling of nebular emission from different gas components ionized by different sources in simulated galaxies. In this analysis, the methodology introduced by Hirschmann *et al.* (2017) is considered to model in a self-consistent way the nebular emission from different regions in the ISM ionized by various sources in simulated galaxies. This is achieved by coupling photoionization models for AGN (Feltre *et al.* (2016)), young stars (Gutkin *et al.* (2016)) and post-AGB stars (Hirschmann *et al.* (2017)) with cosmological hydrodynamic simulations – both zoom-in simulations of massive galaxies (Choi *et al.* (2017); Hirschmann *et al.* (2017)) and large-scale IllustrisTNG simulations (Pillepich *et al.* (2018); Nelson *et al.* (2018)). The latter provides – for the first time – nebular emission line catalogues of full galaxy populations, allowing for a *first statistical* analysis of the outlined questions.

2. Theoretical framework

2.1. *Cosmological simulations*

Part of the analysis is based on a set of 20 high-resolution, cosmological zoom-in simulations of massive galaxies with present-day halo masses between $7 \times 10^{11} M_{\odot}/h$ and $2.7 \times 10^{13} M_{\odot}/h$, adopting a WMAP3 cosmology (Choi *et al.* (2017); Hirschmann *et al.* (2017)). These simulations were performed with a modified version of the highly parallel, smoothed particle hydrodynamics (SPH) code GADGET3 (Springel, Di Matteo & Hernquist 2005) and SPHGal (Hu *et al.* 2014; Choi *et al.* 2017; Nunez *et al.* 2017).

In addition, the publicly available large-scale cosmological "IllustrisTNG" simulation is employed, providing a box length of 100 Mpc, and adopting a Planck cosmology (Pillepich *et al.* (2018), Nelson *et al.* (2018)). This simulation was performed with the magneto-hydrodynamic code Arepo (Springel *et al.* 2010). Note only galaxies with a stellar mass above $3 \times 10^{9} M_{\odot}$ are considered (due to resolution limits).

For more details on the cosmological simulations, the readers are referred to the original works as cited above.

2.2. *Coupling to Photo-ionisation models*

The re-simulations of 20 galaxies as well as the IllustrisTNG-100 simulation presented in Section 2.1 are post-processed to include nebular emission. Recent prescriptions of Gutkin *et al.* (2015), Feltre *et al.* (2016) and Hirschmann *et al.* (2017) are adopted to compute the nebular emission arising from young massive stars, narrow-line regions of AGN and the environment of post-AGB stars. All emission-line models presented here were computed using version c13.03 of the photoionization co de CLOUDY (Ferland *et al.* 2013).

This extensive grid of nebular-emission models is coupled with the cosmological simulations, by selecting the SF/AGN/PAGB models appropriate for each galaxy by self-consistently matching all model parameters possibly available from the simulations

https://doi.org/10.1017/S1743921320000708 Published online by Cambridge University Press

(e.g. different BH, star and gas properties). Those parameters that cannot be retrieved from the simulation are set to standard values (i.e. ξ_d and n_H).

For more details on the grids of photo-ionisation models and on the coupling methodology, the reader is referred to Hirschmann *et al.* (2017).

3. The [OIII]/Hβ–[NII]/Hα diagram in the low redshift Universe

In this section, optical line-ratios of low-redshift simulated galaxies are explored. Specifically, the top row of Fig. 2 of Hirschmann *et al.* (2017) and the top row of Fig. 1 show the locations of galaxies in the [O III]/Hβ and [N II]/Hα diagnostic diagram for different galaxy types. Thereby, different galaxy types are theoretically distinguished on the basis of the predicted ratio of BH accretion rate (BHAR) to SFR and the Hβ-line luminosity (see Hirschmann *et al.* (2017) for exact definitions). For reference, the location of local ($z \sim 0.1$) SDSS galaxies is indicated in these line-ratio diagrams (black contours), together with standard observational criteria to distinguish SF galaxies (below the dashed line) from composites (between the dashed and dotted lines), AGN (above the dotted line) and LI(N)ER (in the bottom-right quadrant defined by dot-dashed lines), according to Kewley *et al.* (2001); Kauffmann *et al.* (2003).

As already discussed in Hirschmann *et al.* (2017/2019) for the set of zoom-in simulations, the top row of Fig. 1 now *statistically* confirms that, in the low-redshift Universe, simulated galaxies occupy the same areas as SDSS galaxies in the [O III]/Hβ–[N II]/Hα plane. In addition, simulated galaxies of SF, AGN, and PAGB types appear to be located in the same regions of the diagram as the observationally defined SF, AGN, and LI(N)ER classes. Only composite galaxies appear to be distributed more widely than the observations, extending to higher than observed [OIII]/Hβ ratios at the highest AGN luminosities. None the less, the overall agreement between models and observations in Fig. 1 is striking given that, in our approach, different galaxy types are linked to physical parameters, such as the fraction of total Hβ luminosity and the BHAR/SFR ratio.

4. Evolution of the [OIII]/Hβ–[NII]/Hα diagram

Turning towards higher redshifts, the bottom row of Fig. 1 shows the analogue of the first row, but for z=3. As expected from the evolution of the 20 re-simulated galaxies Fig. 1 in Hirschmann *et al.* (2019), the bottom row of Fig. 1 confirms for a *statistical* population of simulated galaxies that [OIII]/Hβ tends to increase and [NII]/Hα to decrease from low to high redshift – qualitatively consistent with observations by Yabe *et al.* (2014) and Steidel *et al.* (2014). The physical origin of the cosmic evolution [OIII]/Hβ and [NII]/Hα is a complex mix of different evolving ISM and ionizing-radiation properties governing the nebular emission from young stars, AGN and post-AGB stars (see Hirschmann *et al.* (2017) for a more in-depth discussion).

In addition, the drop in [NII]/Hα from low to high redshifts makes the different galaxy types less distinguishable towards high redshift, implying that the traditional optical selection criteria become less reliable. The main reason for composite/AGN galaxies to move towards the SF region in the [OIII]/Hβ–[NII]/Hα plane is the lower typical metallicity of high- redshift compared to low-redshift galaxies. But note that the validity of standard optical selection criteria can be preserved by focusing on pre-selected subsamples of metal-rich galaxies at any redshift (see Hirschmann *et al.* (2017)).

5. UV diagnostic diagrams to identify the main ionising sources of metal-poor galaxies

This section is focused on diagnostic diagrams based on rest-frame UV emission lines to discriminate between ionizing sources in metal-poor galaxies at high redshifts

https://doi.org/10.1017/S1743921320000708 Published online by Cambridge University Press

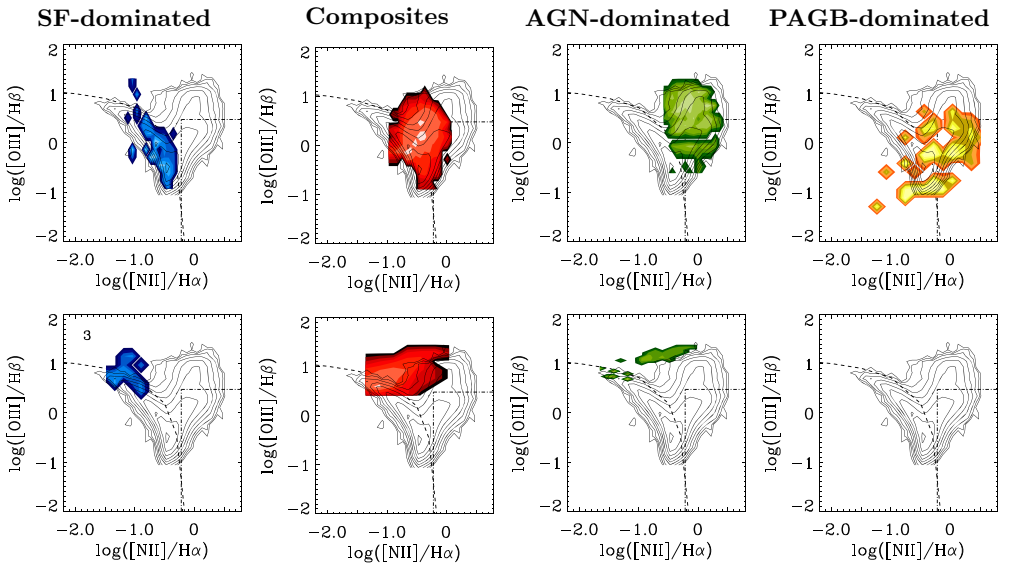

Figure 1. Location of optical line-ratios of IllustrisTNG-100 galaxies in the the [OIII]/Hβ–[NII]/Hα diagram at z = 0 (top row) and z = 3 (bottom row), distinguishing between different galaxy types (blue: SF-dominated, red: composites, green: AGN, yellow: PAGB-dominated).

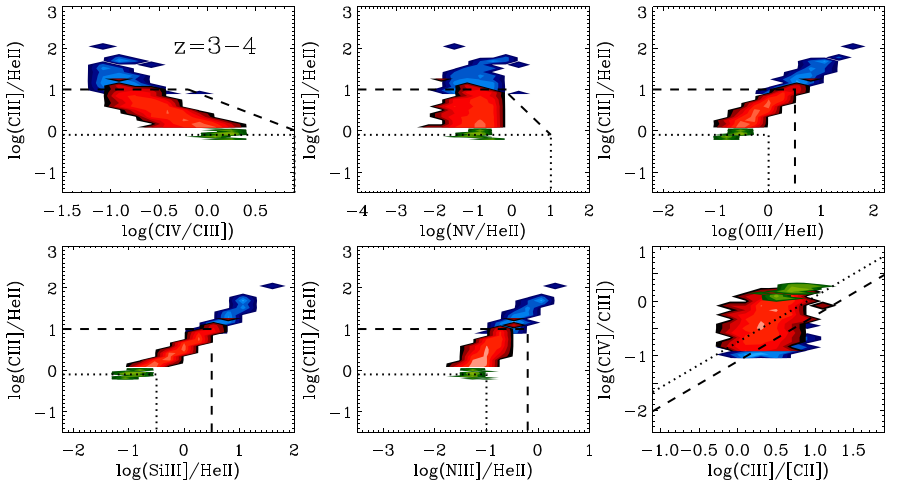

Figure 2. Six UV diagnostic diagrams for metal-poor galaxies of the IllustrisTNG-100 simulation at z = 3-4, distinguishing between SF-dominated (blue), composite (red) and AGN-dominated galaxies (green).

(where optical diagnostics become less reliable). Specifically, the usefulness of different combinations of UV line ratios, proposed by Hirschmann *et al.* (2019), are studied in a *statistical context*. Fig. 2 shows six (out of the 14 proposed) different UV diagnostic diagrams of metal-poor galaxies at z = 3-4, distinguishing the nature of the main ionising sources according to the BHAC/SFR ratio (as in section 3): (i) CIII]λ1908/HeIIλ1640 versus CIII]λ1908/CIVλ1550; (ii) CIII]λ1908/HeIIλ1640 versus NVλ1240/HeIIλ1640; (iii) CIII]λ1908/HeII λ1640 versus OIII]λ1663/HeIIλ1640; (iv) CIII]λ1908/HeIIλ1640 versus SiIII]λ1888/HeIIλ1640; (v) CIII]λ1908/HeIIλ1640 versus NIII]λ1750/HeIIλ1640; (vi) CIVλ1550/CIII]λ1908 versus CIII]λ1908/C II]λ2326. The selection criteria, derived

https://doi.org/10.1017/S1743921320000708 Published online by Cambridge University Press

in Hirschmann *et al.* (2019), are indicated by the black dashed (to separate SF from composite galaxies) and by the black dotted lines (to distinguish between composite and AGN-dominated galaxies). Except for the bottom right UV diagram, the separability of different types of metal-poor galaxies in the other UV diagnostic diagrams is fairly clear for the statistical metal-poor galaxy populations.

6. Conclusions

This article is dedicated to the exploration of optical and UV emission-line diagnostic diagrams over cosmic time. As described in Hirschmann *et al.* (2017/2019), synthetic optical and UV emission lines of galaxies have been computed in a cosmological framework by coupling in post-processing newly developed spectral evolution models, based on photoionization calculations, with a set of 20 high-resolution cosmological zoom- in simulations of massive galaxies and, for the first time, with the large-scale cosmological IllustrisTNG simulation. The latter allows for a *statistical* investigation of optical and UV line-ratios of *full* galaxy populations. The following results can be summarised:

- The synthetic [OIII]/Hβ and [NII]/Hα emission-line ratios predicted by the simulations are in excellent agreement with observations of both star-forming and active SDSS galaxies in the local universe.
- Towards higher redshifts [OIII]/Hβ is predicted to increase and [NII]/Hβ to decrease qualitatively consistent with recent observations. The latter makes the standard optical selection criteria in the [OIII]/Hβ–[NII]/Hα diagram less reliable, at least for metal-poor galaxies.
- To robustly classify the ionizing radiation of metal-poor galaxies, which dominate in the early Universe, we can statistically confirm some of the UV diagnostic diagrams and corresponding selection criteria introduced by Hirschmann *et al.* (2019).

Despite these promising results, it is important to keep in mind that a self-consistent relative contribution by radiative shocks to UV- and optical-line ratios is neglected so far, which I intend to add in future work. In addition, I plan to explore the contribution by different ionizing sources to nebular emission in different regions of a galaxy, i.e. producing spatially resolved emission-line maps to improve the interpretation of modern integral-field spectroscopic observations in terms of galaxy physical parameters.

References

Berg, *et al.* 2016, *ApJ*, 827, 126
Choi, *et al.* 2017, *ApJ*, 472, 2468
Feltre, *et al.* 2016, *MNRAS*, 456, 3354
Gutkin, *et al.* 2016, *MNRAS*, 462, 1757
Hirschmann, *et al.* 2017, *MNRAS*, 472, 2468
Izotov, *et al.* 1999, *ApJ*, 511, 639
Kauffmann, *et al.* 2003, *MNRAS*, 346, 1055
Kewley, *et al.* 2001, *ApJ*, 556, 121
Kewley & Ellison 2008, *ApJ*, 681, 1183
Maiolino, *et al.* 2008, *A & A*, 488, 463
Morisett, *et al.* 2016, *A & A*, 594, A37
Nelson, *et al.* 2018, *MNRAS*, 475,624
Pillepich, *et al.* 2018, *MNRAS*, 473,4077
Shapley, *et al.* 2015, *ApJ*, 801, 88
Stark, *et al.* 2014, *MNRAS*, 445, 3200
Steidel, *et al.* 2014, *ApJ*, 795, 165
Strom, *et al.* 2017, *ApJ*, 836, 164
Yabe, *et al.* 2014, *MNRAS*, 437, 3647

https://doi.org/10.1017/S1743921320000708 Published online by Cambridge University Press